

# Ultrahigh vacuum gauges

*K. Jousten*

Physikalisch-Technische Bundesanstalt, 10587 Berlin, Germany

## Abstract

Ionization gauges exclusively are used for ultrahigh vacuum. After a brief history, the design, use, and accuracy of ionization gauges will be described in this article.

## 1 Introduction

In the ultrahigh vacuum (UHV) regime it is not possible to measure pressure as a force on a certain area as the definition of pressure indicates. Instead, it turns out that the only practical and economically reasonable indicator for pressure in UHV is the ionization rate produced by electrons hitting the neutral gas atoms in a UHV chamber (Fig. 1).

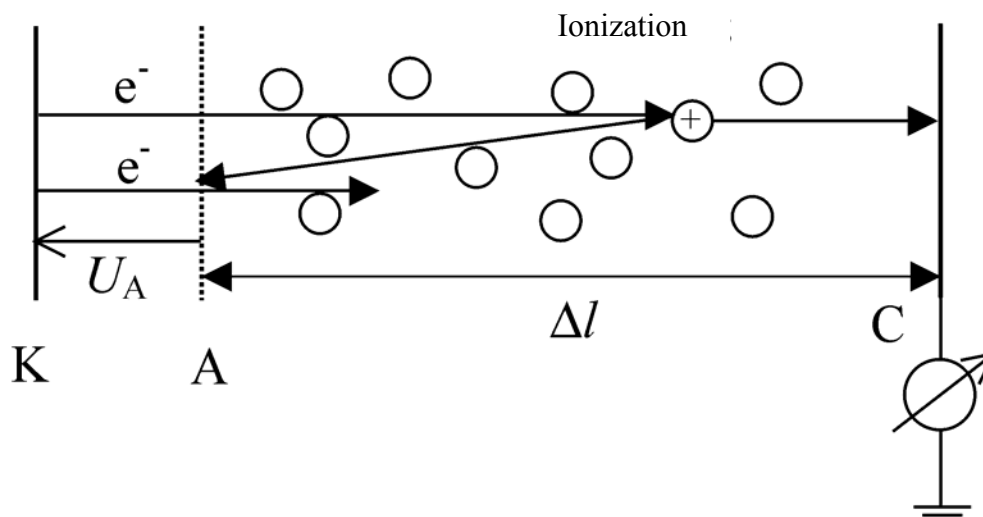


**Fig. 1:** The basic measuring principle of ionization gauges with electron emitting cathode K. Electrons hitting neutral molecules closely enough may ionize them. The ions are drawn to the collector C, the electrons finally reach the anode A.

In such ionization gauges (IG) the ionization rate is proportional to the particle density  $n$  in the gauge volume. Therefore it is important to remember the ideal gas law for an enclosed system in equilibrium

$$p = nkT . \quad (1)$$

It is not sufficient to measure  $n$  with an ion gauge; the temperature  $T$  of the gas also has to be known to indicate pressure with an IG.

Though, in principle, it is also possible to ionize neutral gas molecules by photons (high-intensity lasers) or ions, only the use of electrons is economically feasible. The production method of electrons, however, has generated two main types of ionization gauges: when the electrons are

generated by an electrical discharge, the gauges are usually called ‘cold cathode gauges’, and when the electrons are generated by a heated cathode, they are called ‘hot cathode ion gauges’.

In this article as in newer text books we prefer to call gauges where the electrons are produced by a discharge, crossed field gauges, and where an electron-emitting (i.e., hot) cathode is used, ionization gauges with emitting cathodes. The reason is that nowadays cold emitting cathodes also exist and may in the future come into practical use.

The left branch of Fig. 2 in the article “Gauges for fine and high vacuum” in the mentioned book gives an overview of the classification of the most well-known types of ionization gauges according to their measurement scheme, which will be explained step by step further on in this article.

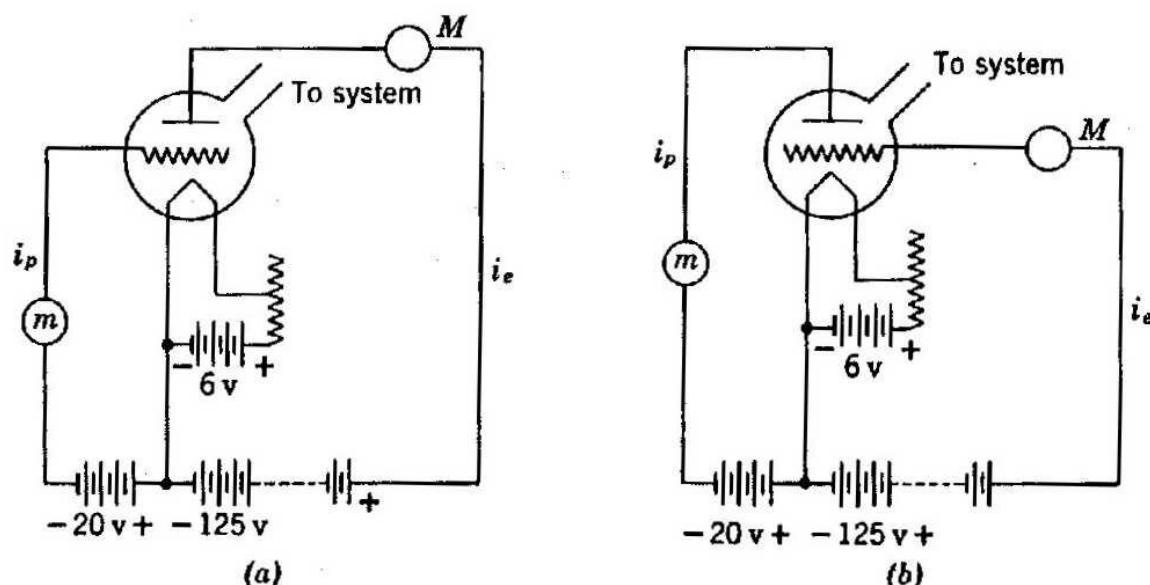


**Fig. 2:** Electrical circuits for historical triode ionization gauges: (a) Internal control type. (b) External control type. From Saul Dushman and J.M. Lafferty, *Scientific Foundations of Vacuum Technique*, 2nd ed., John Wiley & Sons, New York, 1962.

## 2 Brief historical review

The history of the IG dates back to 1909, when Baeyer [1] showed that a triode vacuum tube could be used as a vacuum gauge. However, Buckley [2] is usually recognized as the inventor of the triode gauge. He later improved the gauge to a lowest pressure measurement limit of about  $10^{-6}$  Pa.

Three electrodes, sealed in a glass bulb, were needed for an IG: the cathode, as the source of electrons, the anode, and the collector of positive ions (Fig. 2).

It was possible to use the grid as ion collector as shown in Fig. 2(a), but to use the anode plate as collector, Fig. 2(b), was customary because it was more sensitive. More ions were collected.

A few basic ideas shown in Fig. 2 are identical in today’s gauges. That is, the ion collector has to be negative with respect to the cathode, so as to pick only ions and no electrons, and the acceleration voltage for the electrons has to be roughly 100 V. The reason is that the ionization probability of a neutral gas molecule by an electron is energy dependent and, close to 100 eV, there is a maximum for most gases as can be seen on Fig. 3.

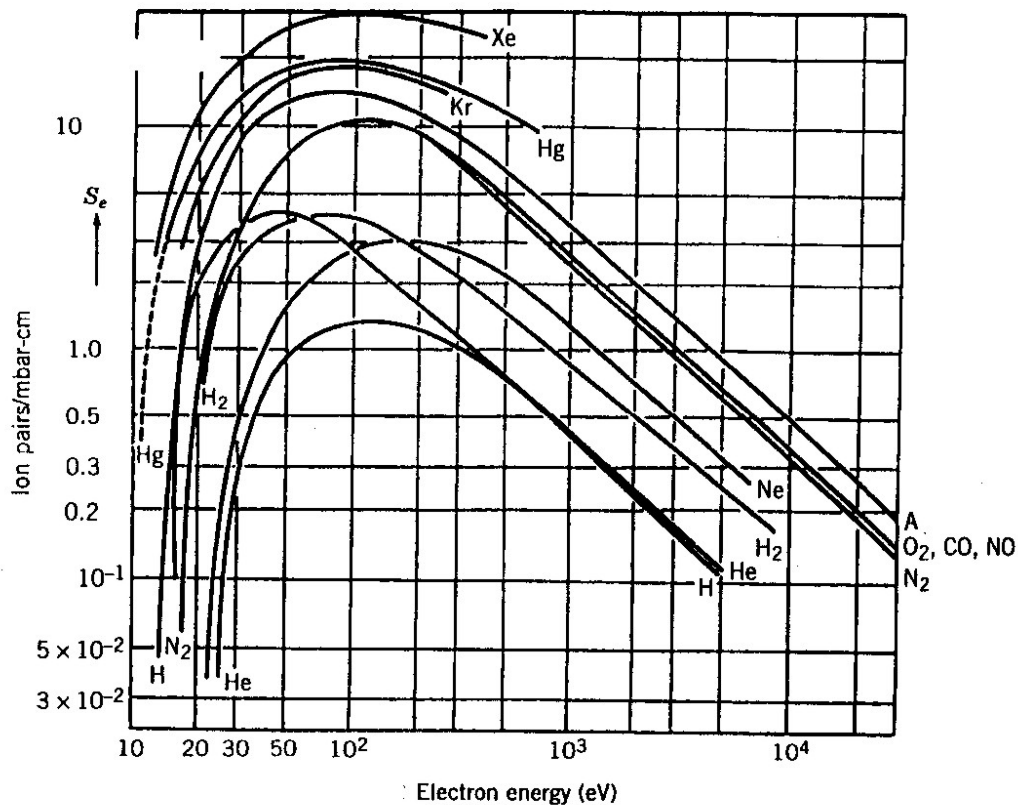


**Fig. 3:** Generated ions per centimetre electron path length per millibar at 20°C versus kinetic energy of incident electrons for various gases. From A. von Engel, *Ionized Gases*, AVS Classics Series.

Because the electron energy should be high on the total path length, the acceleration voltage is usually tuned somewhat higher than 100 V. This also has the advantage that the ionization cross-section differences between different gases are less emphasized.

The basic design of the triode gauge remained unchanged for more than 30 years, although physicists wondered why all vacua stopped at about  $10^{-6}$  Pa. The pumps improved continuously and in the 1930s and 40s there was considerable evidence from measurements of the rate of change of surface properties like the work function and thermionic emission that much lower pressures were actually obtained than were indicated by the IG.

At the 1st International Vacuum Congress (IVC) in 1947 Nottingham suggested that the limit to the lowest measurable pressure was not caused by the pumps, but by an X-ray effect in the IG: he proposed that soft X-rays, produced by electrons impinging on the anode, released photoelectrons from the ion collector; this photocurrent was indistinguishable in the measuring circuit from the current due to positive ions arriving at the ion collector. This hypothesis was soon confirmed by Bayard and Alpert [3] who reduced the size of the ion collector from a large cylinder surrounding the other electrodes to a fine wire on the axis of a grid anode. This elegant solution reduced the lowest measurable pressure by a factor of 100 and is still the most common design in today's commercial IG: the Bayard–Alpert gauge or just BA gauge.

Penning is known as the inventor of the first crossed field gauge [4]. One of the crossed-field gauge types is named after him. His invention was based on an earlier patent by himself for coating by sputtering. It turned out that the discharge current was almost linearly proportional to the pressure in the gauge from 1 mPa to 0.1 Pa.

Figure 4 shows the electrode arrangement, fields, and trajectories in the Penning gauge of 1949 where the anode was changed from a ring in his original version to an open cylinder. This geometry is now widely used in ion pumps, but only for rugged and simple vacuum gauges.

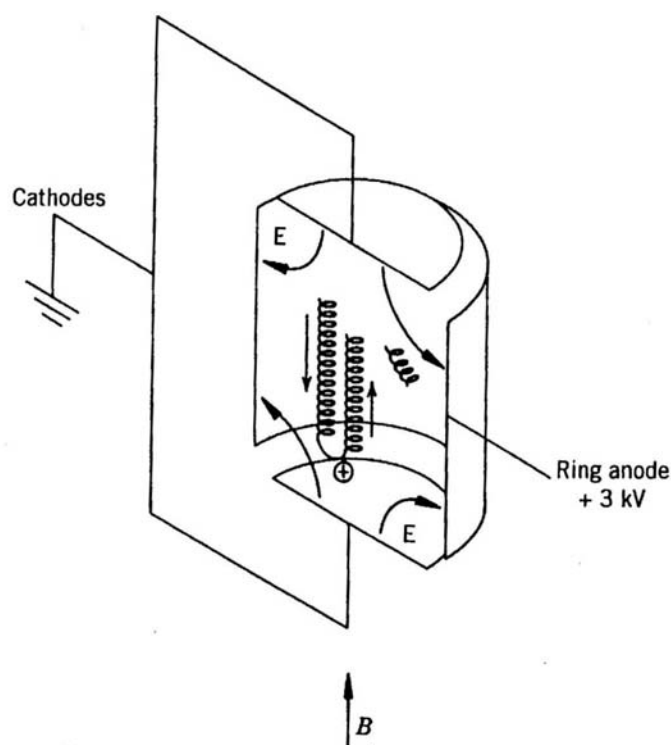


**Fig. 4:** Electrode arrangement, fields, and trajectories in the Penning gauge. From James M. Lafferty, *Foundations of Vacuum Science and Technology*, John Wiley & Sons, New York, 1998.

### 3 Crossed field gauges

#### 3.1 The Penning gauge

The working principle of this type of gauge is to generate a discharge between two metal electrodes (anode and cathode) by applying a DC high voltage. The discharge current is pressure dependent and serves as measurand for pressure. The lower measurement limit lies around 1 Pa, since at lower pressures the gas density is too low to generate enough charge carriers to maintain the discharge.

To extend this limit, a magnetic field crossing the electrical field is used. This magnetic field greatly increases the path length of the electrons from cathode to anode, so that the electron can generate another electron by impacting on a gas molecule to maintain the discharge (Penning discharge). Owing to their higher mass the ions are only slightly affected in their trajectories by the magnetic field and travel directly to the cathode. Secondary electrons released when the ions hit the cathode (cathode sputtering) support the discharge.

In crossed field gauges, the ion current vs. pressure relation follows the equation

$$I^+ = K \cdot p^m, \quad (2)$$

where  $m$  depends on the type of gauge and varies between  $m = 1 \dots 1.4$ .

The mode of operation in a Penning discharge is explained by Fig. 5 and Fig. 6. The case *G* of the Penning gauge is metal and on ground potential. Figure 7 shows a typical calibration curve of such a gauge. It can be seen that there exist two main modes of discharge with the transition around  $10^{-4}$  mbar ( $10^{-2}$  Pa).

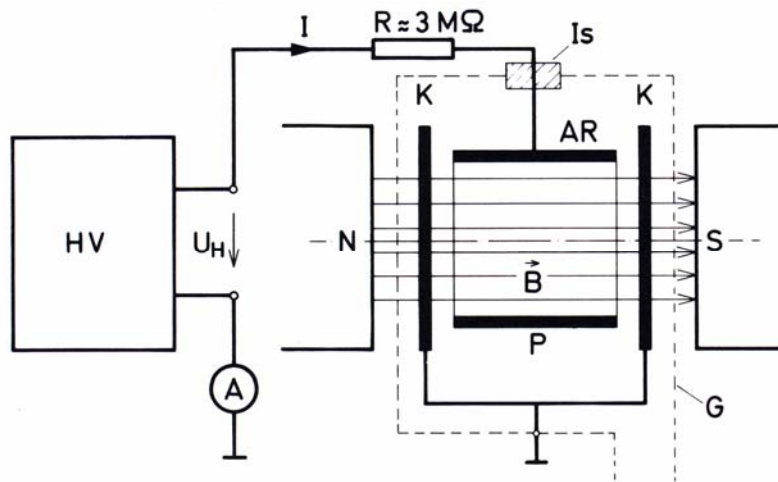


**Fig. 5:** Penning gauge: AR anode ring, K cathode, G case, N, S north and south pole of magnet, HV high voltage. From *Wutz Handbuch Vakuumtechnik* by K. Jousten (ed.), Vieweg Verlag.

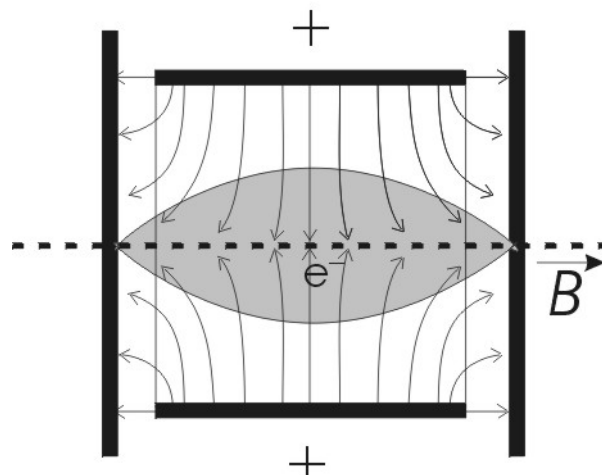


**Fig. 6:** Direction (not strength) of the electrical field in the Penning gauge as in Fig. 5. Grey: electron space charge. From *Wutz Handbuch Vakuumtechnik* by K. Jousten (ed.), Vieweg Verlag.

At low pressures, there is a rotating electron current of about 1 A symmetrical to the axis of the anode cylinder and perpendicular to the magnetic field (grey area in Fig. 6). Between this electron space charge and the anode there is a strong electric field and almost all of the full voltage drops between the space charge and the anode cylinder. For this reason the electrical field gets a strong radial component. Close to the axis of the cylindrical anode a plasma with equal negative and positive charges exists. The electron ring current would be completely stable, if no gas molecules were there. The electrons interact with them in two ways. They hit them with small energy and diffuse out of the electron space charge or they hit them with higher energy and ionize the molecule. In the latter case the new electron will be incorporated in the ring current, the ion will be accelerated by the electrical field and finally reach the cathode. Since both the ionization rate and the diffusion effect (diffusion coefficient) are proportional to the gas density  $n$ , in equilibrium the ring current will be such that the loss of electrons by diffusion is compensated by the generation due to ionization. This means that the

ring current will be roughly independent of  $n$  and  $p$ . For this reason, the outer discharge current will be proportional to  $n$  and  $p$ . The fact that the ring current does slightly increase with  $n$  has as consequence that  $m$  in Eq. (2) is  $> 1$ .

At higher pressures, the positive ion charge becomes so high that the ring current described above will no longer be stable. Instead, an equipotential plasma will build up in the whole space of the anode cylinder with respective space charges opposed to the two electrodes. Ions accelerated onto the cathode generate secondary electrons that compensate the loss of electrons by diffusion to the anode. This diffusion mechanism is amplified by plasma oscillations. In this regime the discharge current is no longer proportional to pressure (Fig. 7).

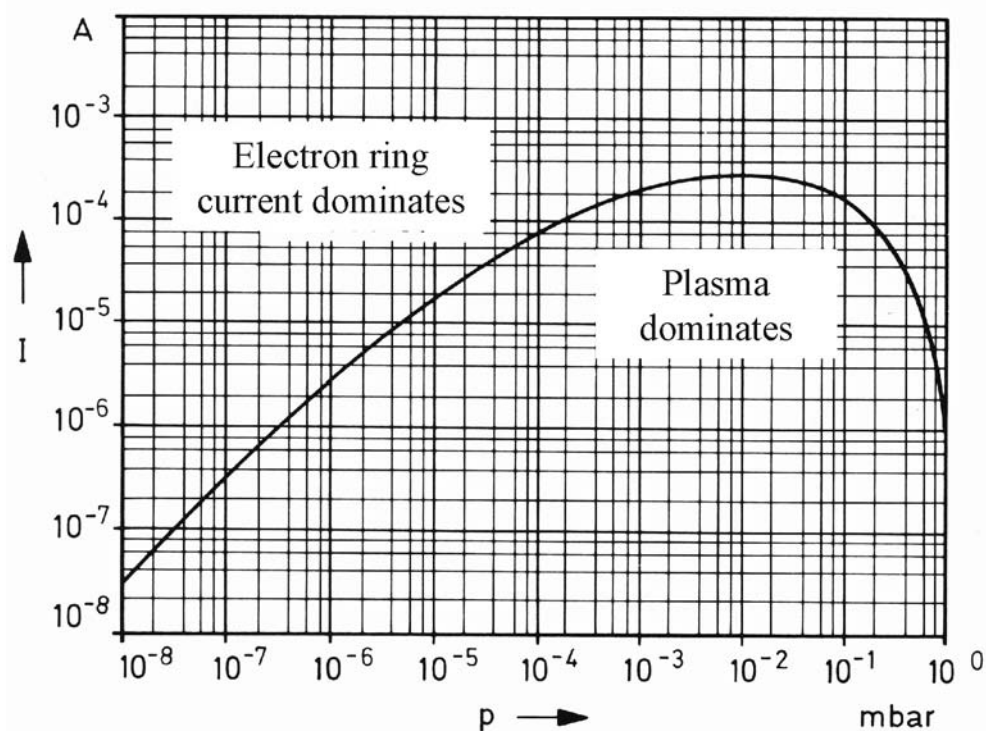


**Fig. 7:** Typical calibration curve of a Penning gauge. From *Wutz Handbuch Vakuumtechnik* by K. Jousten (ed.), Vieweg Verlag.

At high pressures the cathode erodes and the production of secondary electrons depends on the surface of the cathode and it has to be cleaned quite often to get reproducible results.

Since the ring current of a Penning gauge is very high (1 A or so), it has a high sensitivity and the discharge current may be inexpensively measured without an amplifier down to  $10^{-4}$  Pa.

The discharge is generally not stable in crossed field gauges. In the early designs the discharge became erratic below  $10^{-3}$  Pa, and was often extinguished completely at  $10^{-4}$  Pa.

Therefore better designs were invented with the aim of increasing the active volume of the discharge and reducing discontinuities.

### 3.2 Magnetron and inverted magnetron

A kind of breakthrough was accomplished by Redhead and Hobson, who invented and improved the so-called magnetron and inverted magnetron gauge, the latter designed earlier by Haefer in 1955.

In the magnetron gauge [5] (Fig. 8) the anode is an open cylinder with the cathode on axis and as endplates, in the inverted magnetron gauge [6] (Fig. 9) the anode is a rod in the axis of an almost

closed cylinder as cathode. In the magnetron gauge, the end discs of the of the cathode are shielded from high electric fields by two annular rings held at cathode potential. Any field emission that can occur from the shield electrodes is not measured by the ion current amplifier. Versions of the magnetron have been used in satellites and on the surface of the moon in 1969 on Apollo 12 and subsequently also on Apollo 14 to 16 [16].

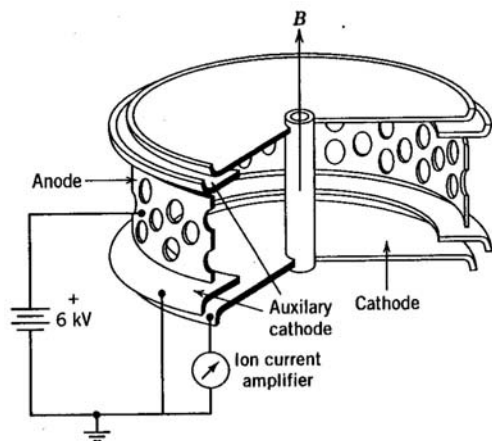


**Fig. 8:** Schematic diagram of the magnetron gauge. From Ref. [5].

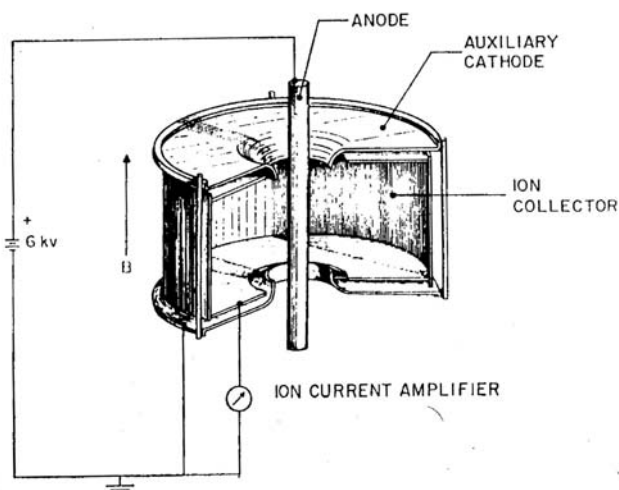


**Fig. 9:** Schematic diagram of the inverted magnetron gauge. From Ref. [6].

One of the important features in the inverted magnetron gauge (IMG) is the use of guard rings held at cathode potential to prevent field emission currents from the cathode to the anode. The magnetic field is parallel to the anode axis. This gauge can be operated up to 6 kV with 0.2 Tesla.

In these gauges the electrons are trapped more efficiently than in the original Penning design. Because of this, the starting conditions are improved, the relations between  $p$ ,  $B$ ,  $V$  follow reasonably the theoretical predictions, and the discharge is stable to much lower pressures. Redhead and Hobson claimed that their gauges could be used from  $10^{-11}$  Pa up to  $10^{-2}$  Pa.

Almost all available commercial crossed field gauges are of the Penning design or of the Redhead and Hobson design as magnetron or inverted magnetron. Normally, at low pressures, the gauges are operated with constant voltage, measuring the discharge current, while at higher pressures ( $> 10$  mPa) they are operated at constant discharge current with accordingly reduced voltages. Otherwise, at constant voltage, the discharge current would be so high at higher pressures that heating and sputtering of material on the electrodes becomes a problem.

However,  $m$  also depends on pressure (Fig. 7) and this makes the situation rather complicated for reliable measurements. Generally,  $m$  is higher for lower pressures than for higher and may reach values up to 2 in extreme cases. If therefore in gauge controllers the relation for higher  $p$  is extrapolated to very low pressures ( $< 10^{-7}$  Pa), the gauge will indicate at these small pressures lower pressures than actually present. At pressures of  $10^{-10}$  Pa this error may be as high as an order of magnitude.

More detailed theoretical descriptions of the characteristics of crossed field Townsend discharges including electron space charge, which controls the discharge, have been given than described in the previous section. However, Redhead [7] has pointed out that these theories have ignored the dynamics of dense electron space charge. The long trapping times of electrons allow large-amplitude rf oscillations to build up. These oscillations modify the static characteristics of the

discharge and low frequency instabilities which are associated with mode-jumping of the rf oscillations. Owing to interaction of the electrons with the produced AC fields, excess energy electrons are generated which easily come across the magnetic field and hit the cathodes (Penning gauge) or the cathode end plates (magnetron or inverted magnetron). They falsify the discharge current and ion current, respectively. Since this effect is pressure independent it causes non-linearities in the current pressure curve. The rf oscillations may also cause serious measurement errors if unintentionally rectified in the ion-current amplifier.

In a summary comparison between crossed field gauges and emitting cathode gauges we shall come back to this point.

Kendall [8] has designed an inverted magnetron gauge that is reduced in size and modified in the magnetic field (Fig. 10) in order to reduce the external magnetic field. This may be of interest wherever the magnetic field of a crossed field gauge has undesirable effects on its environment.

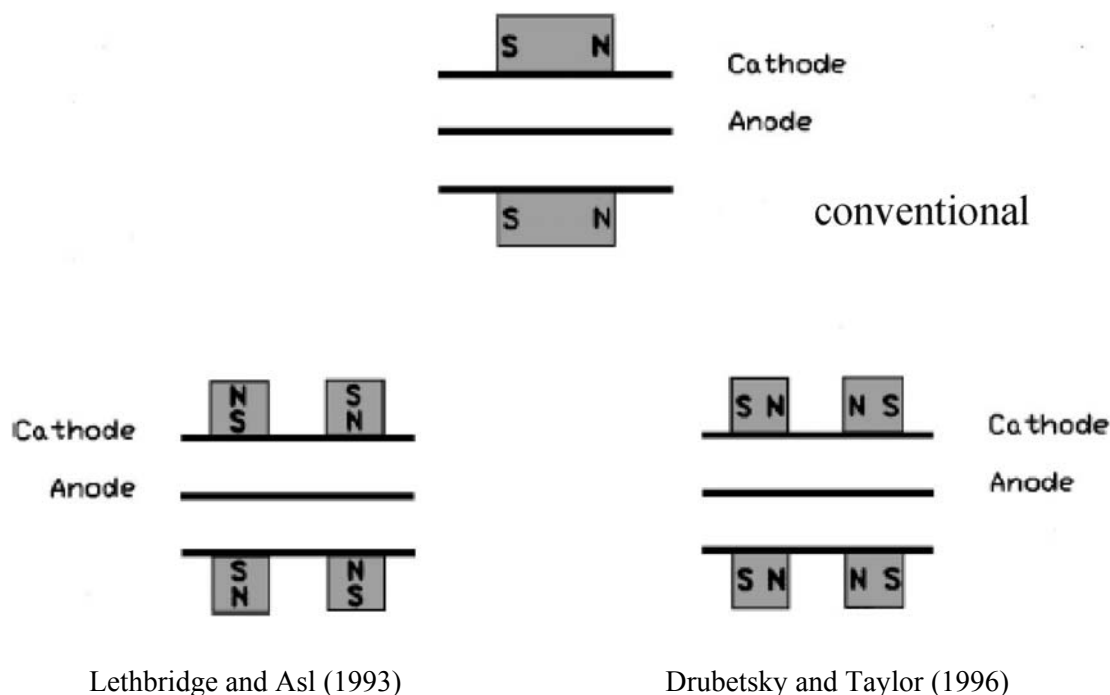


**Fig. 10:** Modified field configuration in an inverted magnetron. From Ref. [8].

#### 4 Ionization gauges with emissive cathodes

In our brief historical review we have already come to the early design of BA gauges and we shall continue from there.

One of the main problems in the beginning of the BA gauge (Fig. 11) was instabilities in the gauge due to the floating potential of the glass envelope. Therefore the glass was furnished with a conductive layer which could be grounded or set on a defined positive potential. Also it was soon noticed that ions could be lost through the open ends of the cylinder and the grid was closed at its ends to reduce this effect. The disadvantage of closing the grid seems to be that the pressure versus ion current ratio becomes non-linear for higher pressures at about 1 mPa, while this is only the case for the open cylindrical grid [9] at pressures of 10 mPa or more.



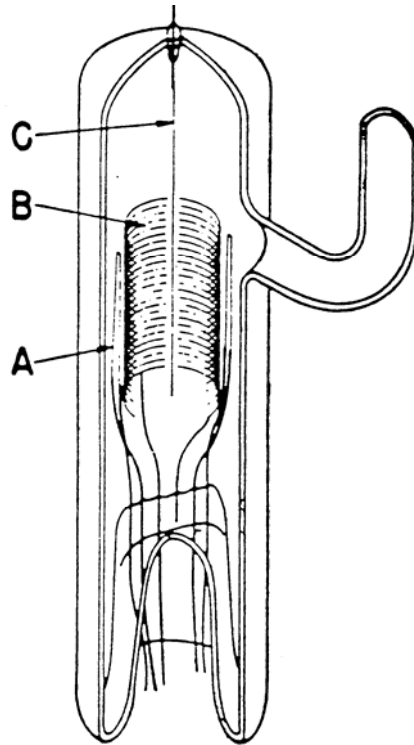


**Fig. 11:** The original design of the Bayard–Alpert gauge. From R.T. Bayard and D. Alpert, *Rev. Sci. Instrum.* **21** (1950) 571.

In order to further reduce the X-ray limit (Fig. 12) there was an attempt to reduce the thickness of the collector wire. For example Van Oostrom [10] reduced its diameter to about  $4\ \mu\text{m}$ . Although with this method the X-ray limit is reduced, theory [11] stated that the sensitivity is also reduced: ions formed inside the grid experience a radially inward force. Since angular momentum must be conserved, an ion with initial kinetic energy may not strike the collector wire, but rather go into orbit around it and tend to drift out axially from the electrode structure. Careful experimental investigations by Benvenuti [12] and Groszkowski [13], however, showed that the variation of collector efficiency with collector diameter was much less than theoretically predicted.

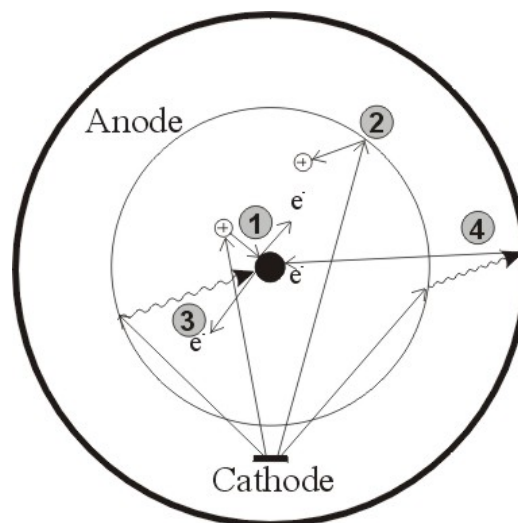


**Fig. 12:** Effects of ionization (1), electron stimulated desorption (2), X-ray effect (3), and inverse X-ray effect (4) in a BA gauge

When the X-ray limit was pushed down in this manner, another component to the background current became evident. Electrons hitting the anode may ionize molecules adsorbed on the surface with a subsequent release (Fig. 12). Ions generated in this manner cannot easily be distinguished from those generated in the gas phase. Since a grid structure of a BA gauge has a surface area of about  $10 \text{ cm}^2$  the amount of adsorbed molecules can be rather high ( $10^{16}$ ). Therefore it is important that the grid structure be very clean. Two measures are usually taken to cure this problem: the grid is cleaned by electron bombardment after the gauge had been exposed to high pressures or the atmosphere, and the electron current to the anode should not be too small during operation so that the gauge is continuously 'self-cleaning'.

To measure pressures lower than  $10^{-9}$  Pa, different approaches have been made.

- The X-ray current is measured so that it can be subtracted from the signal.
- Changes are made in the geometry of the gauge.
- The sensitivity is increased by several orders of magnitude without reducing the background level.

The first two techniques have been found reliable and relatively easy to use in laboratory applications. The third method, however, has been disappointing, because reliable operation could not be demonstrated. Thus, there has been no widespread commercial development.

By using the smallest practical diameter for the collector wire ( $50 \text{ }\mu\text{m}$ ), increasing the sensitivity of the BA gauge by maximizing the volume enclosed by the anode and using end caps, by optimizing the geometry, the materials, the voltages and the emission current, Benvenuti [12] was able to reduce the residual current of the BA gauge (mainly the X-ray induced limit) to the low  $10^{-10}$  Pa regime. The sensitivity of this gauge is higher than  $0.3 \text{ Pa}^{-1}$ . Benvenuti ensured by choosing the right position, shape, and potential of the filament that the electrons cross the grid at right angles in order to maximize their path length and maximize the sensitivity.

The first technique evolved when Redhead [14] suggested ion current modulation by introducing an extra electrode into the grid space. This could be a wire close to the grid and parallel to the collector. When the wire is at grid potential, there is little or no effect on the gauge operation, but when its potential is lowered by 100 V it seriously distorts the ion trajectories, so that the measured collector current is significantly reduced by the so-called modulation index. When this is measured at higher pressures, the residual current due to X-ray effects can be determined at lower pressures.

Most interestingly it was found also that the electron desorbed ions from the grid were modulated [15], [16] and the modulation effect can be used to measure and reduce the electrostatic discharge effect.

It turned out also that the residual current was modulated to a significant extent, because the electron trajectories were also modulated. Hobson [17] estimated that because of this, an error of  $3 \cdot 10^{-10}$  Pa would be introduced in measuring pressure.

Benvenuti again [12], however, demonstrated with his BA gauge with a thin collector wire that a modulation index of 0.9 could be achieved and was able to reach a residual pressure limit  $3 \cdot 10^{-11}$  Pa, one order of magnitude less than predicted. This modulated BA gauge is still in use at CERN and its design has apparently been commissioned first to a French and then to a Swiss company where it is commercially available [18].

Not mentioned so far was the inverse X-ray effect (Fig. 12) which occurs when X-rays hit the enclosure of a gauge and produce secondary electrons that may travel to the ion collector on the same potential and produce a negative current. There were attempts to cancel out the two X-ray effects, but

this is a very unstable situation on account of surface effects. An obvious solution to avoid this effect is to set the collector on a negative potential ( $-30\text{ V}$ ).

The second method of realizing lower pressure measurement led about 30 years ago to the development of the so-called extractor gauge (Fig. 13). In this approach the ion collector is removed out of sight of the grid. A simple lens is introduced between the grid and the collector to pull out the ions to the collector. An ion reflector is used to reflect the ions onto the collector tip to increase the sensitivity similar to that of a conventional BA gauge. In this way pressures from about  $10^{-10}\text{ Pa}$  can be measured. Also in this type of gauge the electrostatic discharge (ESD) effect is greatly reduced. This is because ions released from the grid surface by electron bombardment have sufficient energy to reach the reflector electrode and are not collected.

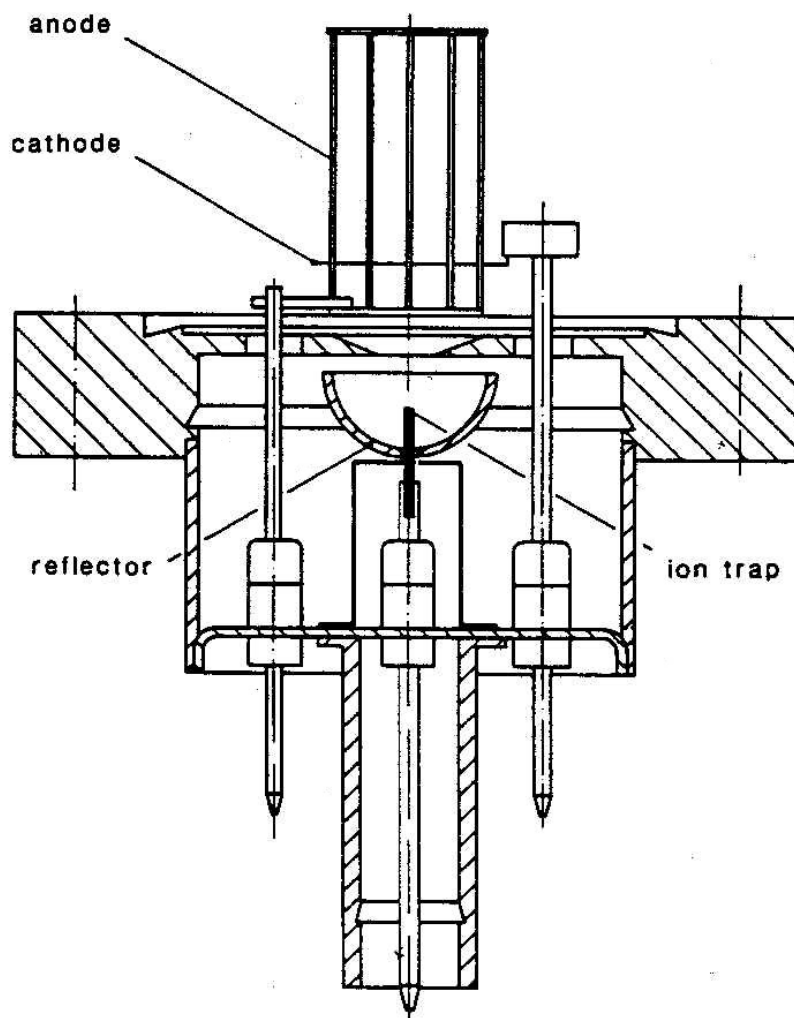


**Fig. 13:** Design of the extractor gauge manufactured by Leybold

This principle of extraction was further developed by Helmer [19]. By shaping the ion beam with a  $90^\circ$  deflector onto the collector there was no line of sight between anode grid and collector (Fig. 14) and the X-ray limit was further reduced to about  $2 \cdot 10^{-11}\text{ Pa}$ . Helmer used a fixed voltage and this was only possible because the energy spread out of a BA gauge (without collector wire in the centre) was found to be unexpectedly narrow (5 eV FWHM) [20]. Since inside the grid the potential varies by about 100 V, this is remarkable. Only due to this narrow energy width was the collection efficiency after the electrostatic analyser high enough.

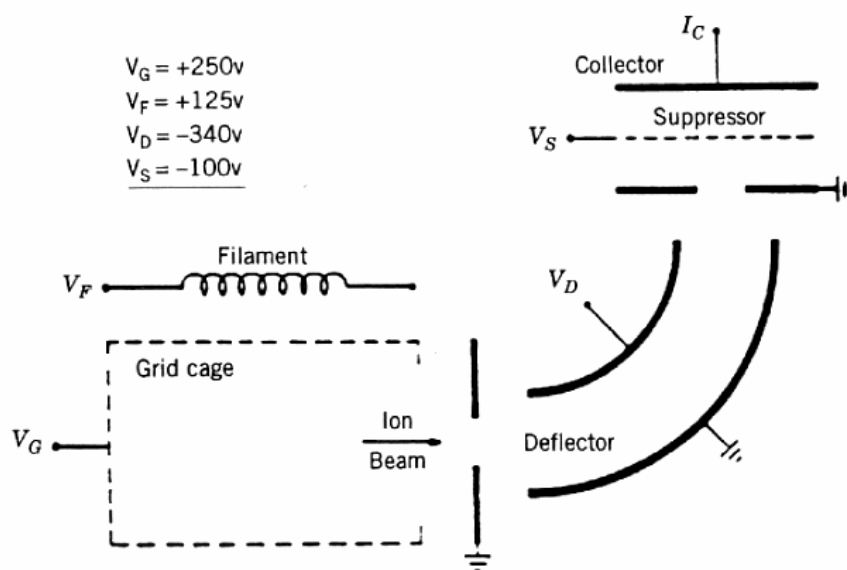


**Fig. 14:** Extractor gauge according to Helmer. From Ref. [19].

Benvenuti and Hauer improved the Helmer gauge by increasing the sensitivity of the ion source and optimizing some geometrical parameters of the extraction [21]. They obtained a residual pressure limit of  $2 \cdot 10^{-12}$  Pa at a sensitivity of  $0.3 \text{ Pa}^{-1}$ . Jitschin [22] used a thoriated tungsten filament and also reduced Helmers limit. B. Lagel at CERN made the latest improvement to the Helmer gauge [23].

A very sophisticated ion gauge was invented by Watanabe in 1992 [24], which he called the ion spectroscopy gauge (Fig. 15).

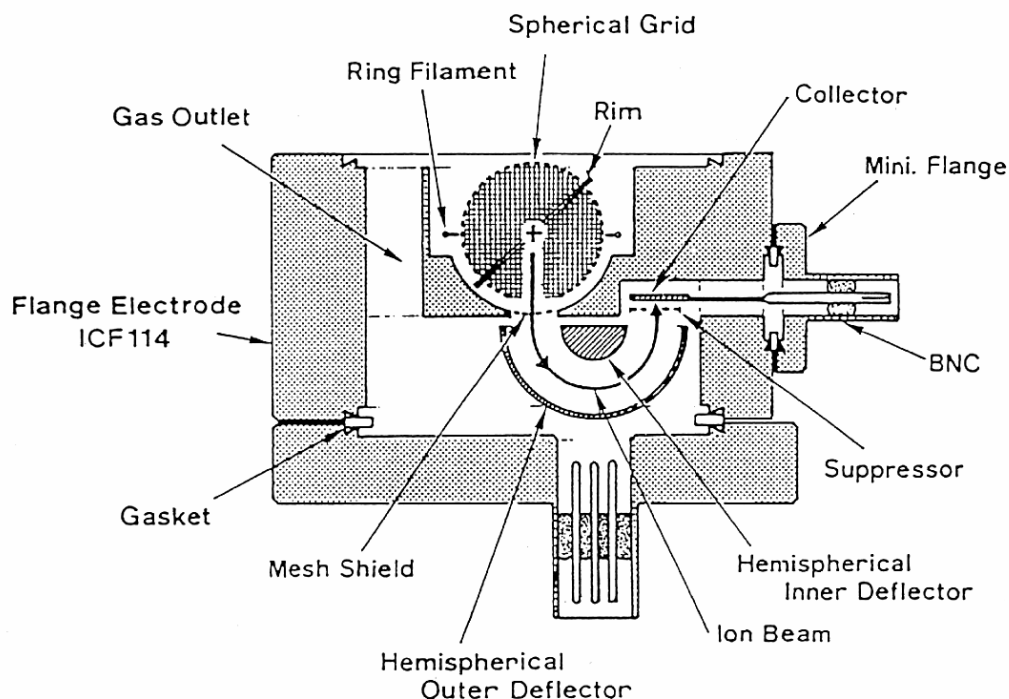


**Fig. 15:** Cutaway drawing of the ion spectroscopy gauge by F. Watanabe. From Ref. [24].

This gauge has so many features that only the most important ones can be mentioned. The gauge uses the extractor scheme, but with a hemispherical deflector so that the ion collector plate is completely out of sight of the grid. The collector is equipped with a suppressor electrode to inhibit electrons which are generated by reflected X-rays leaving the collector. With the hemispherical deflector where the inner electrode is on ground potential and the outer on a variable positive potential, it is possible to separate the ions generated according to their energy. Ions which are generated at the anode grid (electron stimulated desorption effect) have higher energies than ions created in the gas phase because of a potential gradient from the grid to the extractor and because of space charge effects. This effect was also used in the Helmer gauge, but in the ion spectroscopy gauge a spherical grid was used in order to increase the space charge of the electrons in its centre. By this means ESD ions and gas ions can be separated more efficiently than in the Helmer gauge (Fig. 16).

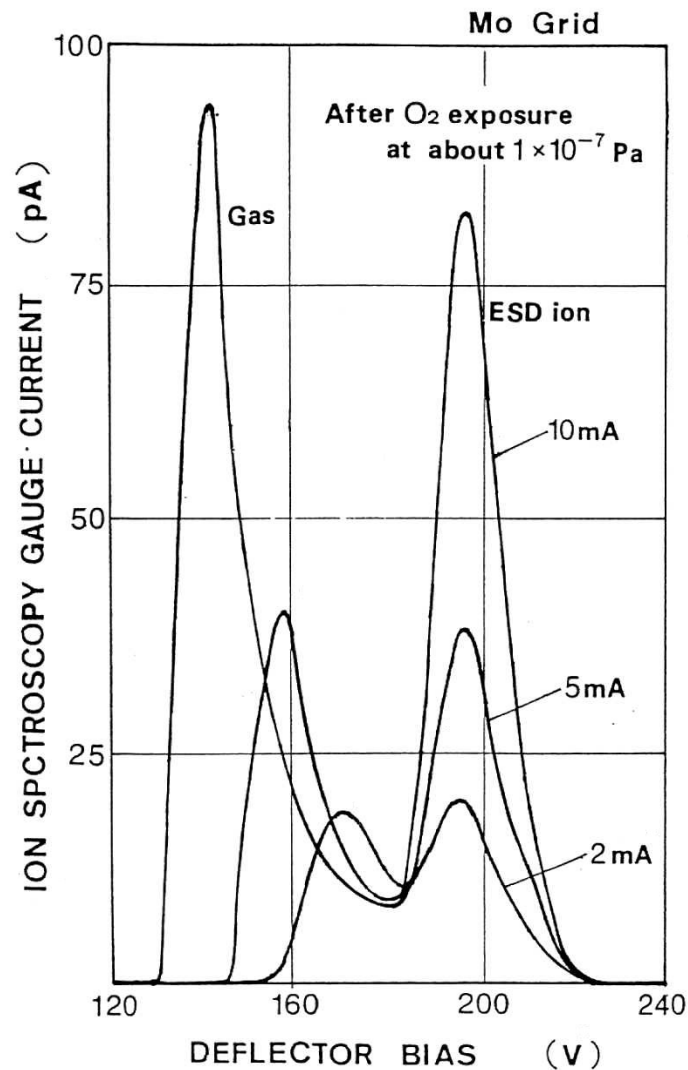


**Fig. 16:** Ion current vs. deflector bias voltage in the ion spectroscopy gauge after oxygen exposure at  $10^{-7}$  Pa. From Ref. [24].

Those parts of the gauge close to the hot filament could be outgassed by resistive heating or electron bombardment. In addition the housing of the gauge was made of high thermal conductance materials such as copper or aluminium in order to reduce the warming up of the gauge, which would stimulate hydrogen outgassing. Watanabe claimed a residual measurement limit of  $2 \cdot 10^{-12}$  Pa for this gauge.

Probably the best known and most successful example for the third method of approaching lower pressure limits is the so-called Lafferty gauge (Fig. 17) [25]. Lafferty adopted the diode magnetron principle by placing the filament along the axis of a cylindrical anode. An axial magnetic field provided by a magnet outside of the enclosure forces the electrons to follow circular paths and increases their path length by orders of magnitude. The electron emission current had to be very low ( $10\ \mu\text{A}$ ) to ensure stable operation. An X-ray limit of about  $3 \cdot 10^{-12}$  Pa was calculated for this gauge.

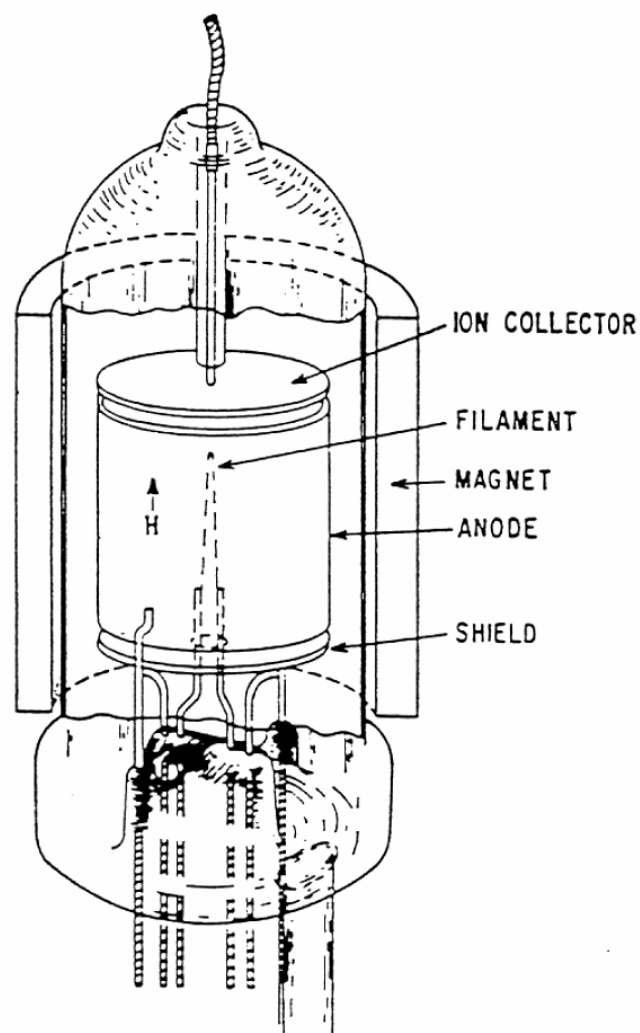


**Fig. 17:** Ionization gauge designed by Lafferty to increase the electron path length. From Ref. [25].

Most of the gauges designed for very low pressures and described above were not commercially successful and are no longer on the market. However, the so-called AxTran gauge (AXial symmetric TRANsmission gauge) [26] by the Ulvac Corporation (Fig. 18) is commercially available. In this gauge the separation between ESD ions and ions generated in free space is provided by an energy analyser called 'Bessel box' [27]. This type of energy analyser is of a straight cylindrical symmetrical design, which has the advantage that the construction of the ion gauge is less space consuming. For a given voltage  $V_{BE}$  only ions around a certain energy may pass the Bessel box and be detected by the secondary electron multiplier (SEM). By optimizing this voltage, ESD ions may be suppressed. In the centre of the Bessel analyser there is a disk with the same potential as the cylinder to avoid a direct line of sight between anode grid and SEM. As lowest measuring limit Akimichi [26] estimated  $3 \cdot 10^{-12}$  Pa, for the commercial instrument it is specified as  $5 \cdot 10^{-11}$  Pa.

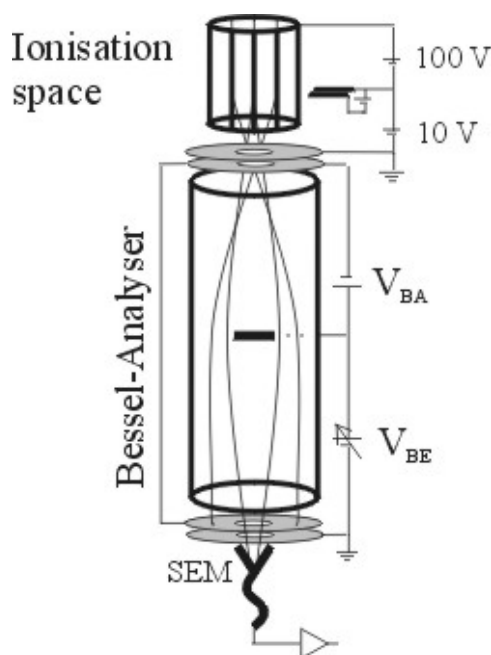


**Fig.18:** Design of the AxTran gauge by Ulvac Co.

There were more approaches to reaching lower pressure limits on all designs of ionization gauges, but the reader should refer to text books or review articles.

So far, only thermionic electron emitting cathodes (hot cathodes) have been described. In the past, field emitter tip arrays of molybdenum or silicon with  $10^4$  tips/mm<sup>2</sup> were developed and used in ionization gauges [28], but the current was only  $20 \mu\text{A}$ . Today the work on cold emitters is still a hot topic and focuses on carbon nanotubes [29]–[33] which can produce current densities of up to  $10^8 \text{ A/cm}^2$  and are commercially used in flat-screen TV sets and miniature X-ray generators. Perhaps carbon nanotubes can replace hot cathodes in the future.

## 5 Comparison of crossed field (CFG) and emitting cathode (ECG) ionization gauges

As a summary, the major types of ionization gauges have been schematically drawn by Redhead (Fig. 19). CFGs have the general advantage that they have no X-ray limit (the electron current producing X-rays is proportional to pressure) and electron stimulated desorption effects are small and cause few errors. Also, because they already have a strong magnetic field, their functionality is less affected by an outside magnetic field than an ECG. In case there is a suitable magnetic field, for example in bending magnets in accelerators, this field can be used for the gauge. On the other hand, for example in electron microscopes, the magnetic field of a CFG may disturb the electron optics and must be carefully shielded.

CFGs have three generic disadvantages:

- Generally their output varies non-linearly with pressure.
- The very dense electron space-charge trapped in these gauges leads to instabilities associated with mode jumping of the high frequency oscillations.
- Their pumping speed is usually one or two orders of magnitudes higher than in ECG and cannot be controlled.

When an ion gauge pumps, this is a classical disturbance effect of a measuring device, because it changes the value of the quantity that it is designed to measure.

The problems in CFGs with starting discharges at low pressures or extinction at low pressures are mostly solved in today's magnetrons or inverted magnetrons by field emitters of radioactive sources built in. It was found by Li [34], however, that the starting time of commercial gauges may largely exceed the manufacturer's specifications.

In ECGs the electron emission current can be controlled, stabilized and varied. Mainly for this reason, ECGs are more stable and accurate, when they are conditioned before measurement.

Li and Jousten [35] have performed a comprehensive study of the stability of CFGs and ECGs with hot cathodes and found that while it is difficult to calibrate CFGs because of the non-linearities and discontinuities, the reproducibility of CFGs is slightly worse than those of ECGs in nitrogen, argon, and helium, but better for hydrogen (Table 1).

**Table 1:** Maximum deviations in per cent from a first calibration run for several gauges (EXG extractors gauge, BAG Bayard–Alpert gauge, IMG inverted magnetron) in different gases over a period of 6 months [35].

	<b>EXG</b>	<b>BAG1</b>	<b>BAG2</b>	<b>IMG1</b>	<b>IMG2</b>
N <sub>2</sub>	-2.5	-4.3	-3.2	-6.2	+5.9
Ar	-1.9	-3.8	+3.8	-2.4	+3.1
He	-5.9	-4.4	-3.6	+8.4	-5.0
H <sub>2</sub>	+9.4	-1.9	-3.6	-1.0	-1.3

When measuring pressures in HV and UHV, one has to decide whether a CFG or a ECG should be bought. For this decision, the following points should be considered.

- Pressure range
- Gauge pumping speed
- Gas species to be measured
- Accuracy and stability
- Size and mechanical stability
- Interferences with magnetic fields
- Price

The available pressure ranges are very much the same for both types of gauge in the sense that there are gauges of either type for very low pressures ( $<10^{-8}$  Pa) and relatively high pressures ( $> 10^{-2}$  Pa). However, the accuracy of ECG is significantly better at very low pressures. An order of magnitude error is easily possible below  $10^{-8}$  Pa [36].

Table 2 and Table 3 give some recent published values [34] of the pumping speed and outgassing rates of some commercial gauges (both CFG and EFG) which were found to be quite consistent with other published data. The pumping speed of a EFG can be reduced by reducing the emission current, but then a complication may arise from the fact that the anode grid is not continuously cleaned by the electrons. As a consequence the ESD effect may increase and disturb measurement.



**Table 2:** Measured pumping speeds in  $\ell/s$  in two inverted magnetrons and two BA gauges, all commercially available. From Ref. [34].

Gas	IMG1	IMG2	BAG1 at 4 mA	BAG2 at 1 mA	BAG2 at 10 mA
N <sub>2</sub>	$4.5 \cdot 10^{-2}$	$6.5 \cdot 10^{-2}$	$1.9 \cdot 10^{-2}$	–	$4.5 \cdot 10^{-2}$
Ar	$2.0 \cdot 10^{-1}$	$2.1 \cdot 10^{-1}$	$6.7 \cdot 10^{-2}$	$3.7 \cdot 10^{-2}$	$2.3 \cdot 10^{-1}$

**Table 3:** Measured outgassing rates in Pa  $\ell/s$  of commercial extractor and BA gauges. From Ref. [34]. The outgassing rate of two inverted magnetron gauges was below the measurable limit.

EXG at 1.5 mA	BAG1 at 4 mA	BAG2 at 1 mA
$2.4 \cdot 10^{-8}$	$8.1 \cdot 10^{-8}$	$3.0 \cdot 10^{-8}$

Hot cathodes are extremely subject to disturbance when gases other than rare gases or nitrogen have to be measured. For in the sense of vacuum science so-called chemically active gases, CFGs should be used which can also be cleaned much easier than ECGs.

The price of a CFG is usually lower than that of an ECG.

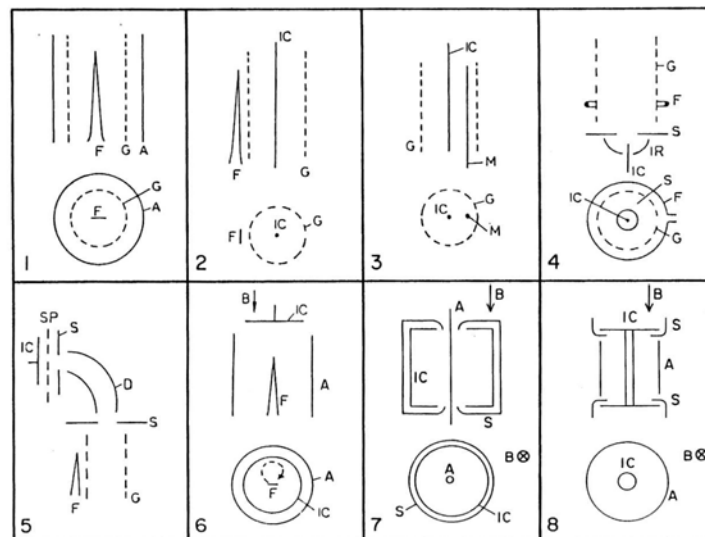


**Fig. 19:** Overview by Redhead of the major types of ionization gauges. 1 conventional triode gauge; 2 Bayard–Alpert gauge; 3 modulated Bayard–Alpert gauge; 4 extractor gauge; 5 bent-beam gauge (Helmer gauge); 6 hot-cathode magnetron (Lafferty gauge); 7 magnetron; 8 inverted magnetron. A-Anode, D-deflector, F-filament, G-grid (acts in 1 as collector), IC- ion collector, IR-ion reflector, M-modulator, S-shield, SP-suppressor.

## 6 Problems in applications of ionization gauges

Special to the application of ion gauges in accelerators are their interaction with radiation, strong magnetic fields, and EM radiation mainly in the radiofrequency range: radiation capable of ionizing molecules may contribute inside the gauge head to the ion current. Miertusova [36] found completely erratic pressure indications when an inverted magnetron gauge was installed very close to a photon absorber. The reason was the characteristic X-ray radiation from copper. Both CFGs and EFGs have to be shielded very carefully from strong magnetic fields in order to get reasonable pressure indications. Hysteresis effects are typical for an incomplete magnetic shielding of CFGs.

Suppose there is a sealed-off chamber at room temperature which is not pumped. An ionization gauge is installed on it to measure the pressure  $p_1$  inside, which we assume as pure hydrogen. Now let us immerse the whole chamber in liquid nitrogen. The pressure will drop by

$$\frac{p_2}{p_1} = \frac{T_2}{T_1} = \frac{77}{300} = 0.257 \quad (3)$$

but the reading of the IG will be unchanged, because the gas density is the same as before. This example shows how important it is to determine also the temperature during a measurement. Even gas temperature variations according to room-temperature variations have to be considered when gauges are accurately calibrated [37].

In other cases, when a chamber is continuously pumped, the molecular flow will adjust such that the law of continuity holds. For example, installing a gauge with hot cathode in a tube (Fig. 20) results in the so-called thermal transpiration effect, where

$$\frac{p_1}{p_2} = \sqrt{\frac{T_1}{T_2}}. \quad (4)$$

Since the hot cathode heats up its enclosure, the temperature  $T_2$  will be larger than in the chamber ( $p_1, T_1$ ) and the pressure  $p_2$  will be accordingly higher, but the reading of the ion gauge will be lower, because  $n_2 = n_1(T_1/T_2)^{1/2}$ .

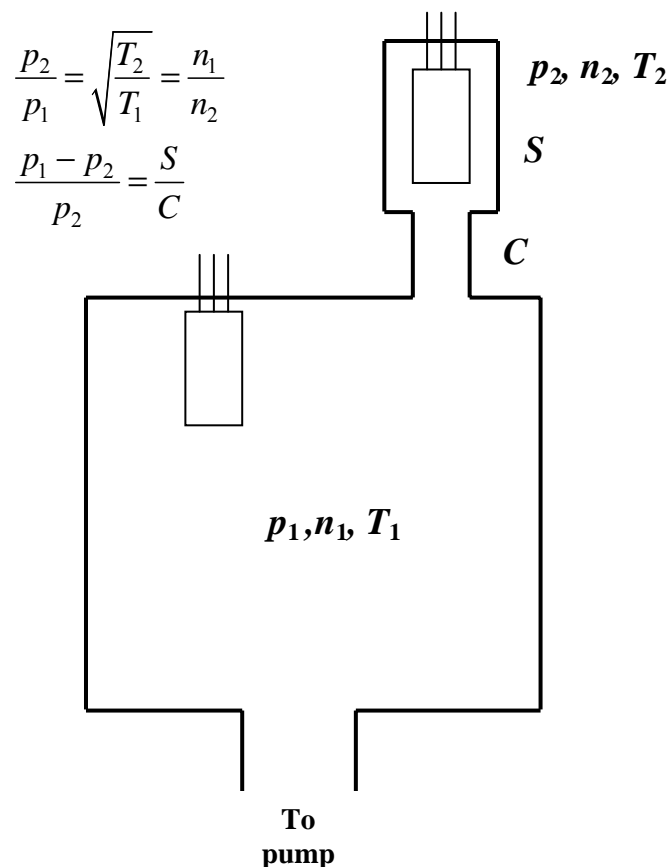


**Fig. 20:** Effects of tubulation of a gauge by conductance, internal pumping speed of the gauge, and thermal transpiration

Another disadvantage of installing IGs in tubes is problems associated with their pumping speed (Fig. 20). All IGs do pump, at least the ionized gas molecules, but pumping effects due to adsorption and dissociation can be much higher. If the conductance of the tube  $C$  to the IG is comparable to the pumping speed  $S$  of the gauge, the pressure in the IG is lower than that at the entrance of the tube.

The advantage of installing a gauge in a tubulation is that the electrical field inside the gauge is not altered by different enclosures. Considerable sensitivity changes can be observed, when gauges are calibrated in the so-called nude configuration (Fig. 20) (no tubulation, but immersed in a large chamber) or in tubes of various inner diameters. Another advantage of tubulated gauges is that they are less sensitive to stray ions from a plasma process or other gauges.

Other problems when measuring pressure are due to non-uniform pressure distributions inside chambers or net fluxes of molecular flow.

Consider the example of Fig. 21, where gas flows from the left to the right and suppose the right wall is a cryo surface with sticking probability = 1. The upper (a) ideal gauge (no internal gas source) will read zero, while in orientation (b) it will read an equilibrium pressure, which is determined by the equality of the rate of influx and the rate of return flow through the tubulation. Neither of these gauges represents the true pressure.

Problems with hot-cathode ionization gauges (HIGs) arise with dissociation and enhanced chemical reactions on the hot cathode surface. For example in tungsten filaments ( $2200^{\circ}\text{C}$ ), there is always carbon present on the surface which diffuses out of the bulk as impurity. Also oxygen is present on its surface. Some reactions which can take place after dissociation of hydrogen are shown in Fig. 22 [38]. It was also reported [39] that at high cathode temperatures hydrogen dissociates and adsorbs on the grid and other parts of the ion gauge. This will also change the sensitivity because of a different reflection coefficient of electrons at the grid. The use of thoriated tungsten or iridium cathodes with operating temperatures of  $1200^{\circ}\text{C}$  avoids this effect.

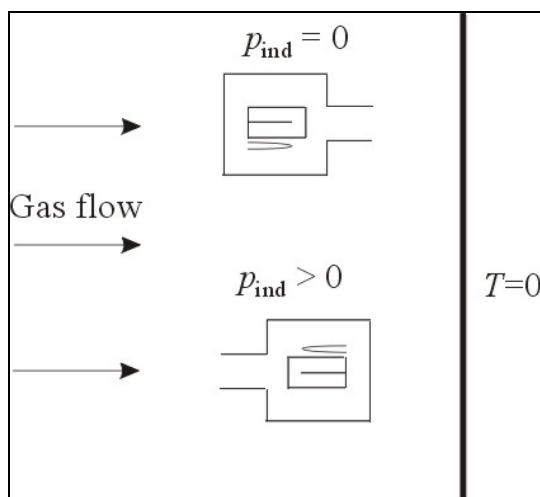


**Fig. 21:** Example of orientation effects when measuring gas pressures with vacuum gauges.  $T = 0$  means in other words a sticking probability of 1.

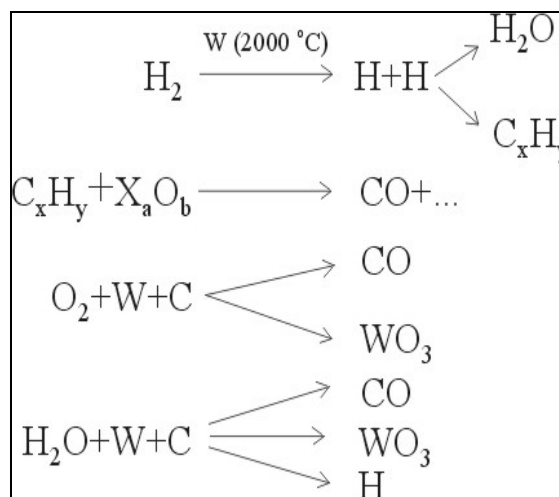


**Fig. 22:** Some chemical reactions which can occur at the hot tungsten filaments in ionization gauges [38]

Outgassing and re-emission of molecules previously pumped by the gauge, is a significant problem in IGs. A gauge operated at higher pressure will have a long relaxation time of hours or days, until a stable pressure at very low pressures is achieved. Outgassing rates of HIGs vary typically from  $10^{-9}$  Pa l/s to  $10^{-7}$  Pa l/s and are often the main source of gas when very low pressures must be achieved.

To get a reliable and long-term stable gauge reading, the gauge electrode surfaces have to have a stable surface structure and composition. Not only does the secondary electron yield on the collector change with the surface composition, but also the number of secondary electrons generated by electrons hitting the anode grid is dependent on the anodes surface composition. Higher energy electrons ( $> 20$  eV) also contribute to the number of ions generated in the gauge, hence the gauge sensitivity.

The gauge sensitivity depends on the gas species. Attempts to correlate this gas-specific sensitivity accurately with ionization cross-sections failed due to other gas-specific effects like ion capture probability, dissociation effects and secondary electron generation. Values for relative ionization sensitivities (normalized for nitrogen = 1) presented in tables (Table 4, [40], [41]) can be applied with some confidence while jumping from one gas to another, but the level of accuracy is only 10–20%. Where greater precision is required, gauges must be calibrated individually and for the gas used in the application.

**Table 4:** Correction factors  $CF$  for different gases when an ionization gauge is set to a correct nitrogen reading. The uncertainty of these values (except nitrogen) is typically 10%, but may be higher in special cases.

<b>Gas species</b>	<b><math>CF_i (N_2)</math></b>
N <sub>2</sub>	1
He	7.24
Ne	4.55
Ar	0.85
Kr	0.59
Xe	0.41
H <sub>2</sub>	2.49
O <sub>2</sub>	1.07
Air	1.02
CO	0.97
CO <sub>2</sub>	0.70
J	0.17
CH <sub>4</sub>	0.71
C <sub>2</sub> H <sub>6</sub>	0.37
C <sub>3</sub> H <sub>8</sub>	0.22
CF <sub>2</sub> Cl <sub>2</sub>	0.36
Oil vapours	0.1

As a final example of what effects have to be considered in a hot-cathode ionization gauge (HIG), calibration results for the sensitivity of H<sub>2</sub> and D<sub>2</sub> should be mentioned. Since the electronic structure of H<sub>2</sub> and D<sub>2</sub> is identical for the purpose of an IG, it could be expected that the relative sensitivity of H<sub>2</sub> to D<sub>2</sub> would be exactly 1. It was found that this is not true and the relative sensitivity varies from gauge to gauge. Moreover, the ratio was not even a constant for a single ion gauge. It varies with the treatment and history of the gauge. This is very surprising, since neither the potentials nor the geometry in the gauge were changed.

The reason for the difference in the sensitivity for H<sub>2</sub> and D<sub>2</sub> is that H<sub>2</sub> because of its smaller mass and higher velocity in the same electric field gives a larger secondary electron yield at the collector than D<sub>2</sub>. This higher secondary electron yield results in a higher current on the collector and therefore a higher sensitivity. The secondary electron yield on the collector depends strongly on the surface condition, so that also explains why the ratio changes with treatments and history of the gauge.

If the secondary electrons are completely pushed back to the collector by applying a negative potential on a suppressor grid in front of the collector, as can be done in the ion spectroscopy gauge of Watanabe, the sensitivity ratio for  $H_2/D_2$  indeed equals 1.

An ECG has to be outgassed when new and after each exposure to atmospheric pressure. This is best done by electron bombardment after a bake-out when the system is still warm. In addition, operation in argon at a pressure of about 1 mPa helps to clean the ion collector.

A safety precaution should be mentioned. During electron bombardment potentials as high as 1000 V are needed in ECGs and a glow discharge may develop and charge up electrodes in the vacuum chamber quite remote from the ECG. This may also happen when operating a CFG. Therefore all parts of a vacuum system (e.g. unused feedthroughs) should be effectively grounded at all times.

## 7 Accuracy and the calibration of ionization gauges

As far as is known to the author, manufacturers calibrate ion gauges in a rough manner for nitrogen before the gauge leaves the factory. This calibration gives you typically an accuracy of within 10% for nitrogen and good quality gauges, for other gas species the accuracy is worse. If better accuracy is required, especially over the lifetime of the ion gauge, it has to be calibrated with a primary standard or a secondary standard for vacuum pressures.

Table 5 and Table 6 list general and specific reasons for measurement uncertainties with ionization gauges. Some of the general reasons have also been mentioned in the section on fine vacuum gauges.

**Table 5:** General reasons for measurement uncertainties with ionization gauges

<b>General reasons for measurement uncertainties</b>
Uncertainties due to calibration chain
Uncertainties due to installation (or mistakes in installation)
Uncertainties due to operation (surface layers, corrosion, dust, ageing)
Inaccuracies caused by gas mixture
Uncertainties caused by the device itself

**Table 6:** Uncertainties that are caused by the individual ionization gauge

<b>Gauge-specific reasons for measurement uncertainties</b>
Offset due to X-ray, ESD, electronics, incomplete insulation
Offset instability (drift)
Resolution
Influences of environment (mainly temperature)
Non-linearity
Integration time (scatter of data), repeatability
Reproducibility (stability of calibration constant)
Hysteresis (ESD)
Prior usage, cleanliness

The calibration constant of an emitting cathode ionization gauge is the so-called sensitivity of an ion gauge. This is defined by

$$S = \frac{I^+ - I_{\text{res}}^+}{I^- (p - p_{\text{res}})} . \quad (5)$$

where  $I^+$  is the collector current at pressure  $p$  and  $I_{\text{res}}^+$  the collector current at the residual pressure  $p_{\text{res}}$  and  $I^-$  is the electron current. Simplifying equations like

$$S = \frac{I^+}{I^- p} \quad (6)$$

should not be used because when  $p$  is so low that  $I^+$  is approaching its lower limit  $I_{\text{res}}^+$  (X-ray limit, electron stimulated desorption and outgassing of the gauge) the sensitivity goes to infinity, which makes no sense (a high sensitivity is usually considered as something desirable).

In CFG the ionizing electron current cannot be measured and in this case the sensitivity is usually defined as [17]

$$S = \frac{I^+}{p^m} \quad (7)$$

where  $m$  is a numerical exponent. This equation for a CFG is more simple than that for ECG [Eq. (5)], because it is assumed that there is no residual collector current (field emission, however, may occur or voltage insulation problems may be present).

It is widely assumed that the collector current of the ECG is strictly linear with pressure, hence that  $S$  as defined in Eq. (5) is pressure independent. This is generally not true as mentioned in Table 6. In cases where high-precision current meters are being used to determine  $S$ , typical relative variations of  $S$  of a few per cent are found. In cases, where lower quality current meters as typical for built-in devices for ion gauge control units are used, differences of  $S$  between different pressure decades of 10% or more can be found. These differences are mainly due to imprecise resistors and rarely due to effects in the gauge itself.

The reason for the gauge-inherent pressure dependence lower than about 1 mPa is unknown, but several effects could be responsible: space-charge effects may vary with pressure, secondary electron yield on the collector can be pressure dependent, and also the electron emission distribution from the cathode may be pressure dependent [42]. Above about 10 mPa it can be expected that the sensitivity will be pressure dependent because of intermolecular collisions and ion-neutral collisions, but also because of changes in space charge [43].

The accuracy of pressure measurement with calibrated ionization gauges is mainly determined by long-term instabilities of their sensitivity. Typically, high quality BA gauges have long-term instabilities of between 2% and 5%.

Two basic calibration methods exist for the calibration of ionization gauges: the calibration by comparison with a reference gauge or the calibration on a primary standard for high and ultrahigh vacuum pressures.

The calibration by comparison is the less accurate method, mainly because the measurement uncertainty and the long-term instability of the calibrated reference gauge has to be taken into account. The calibration by comparison has to be carried out in an apparatus that ensures that the pressure and gas density are the same at the position of the test gauge and the reference gauge. In the review [44],

systems for calibration by comparisons have been described. If available, it is recommended that a spinning rotor gauge be used for the calibration of an ionization gauge between  $3 \cdot 10^{-4}$  Pa and  $10^{-2}$  Pa, because it is much more accurate than the calibration with an ionization gauge on account of the better stability of the spinning rotor gauge compared to the ionization gauge.

The calibration of an ionization gauge on a primary standard is the most accurate calibration method because a primary standard has the highest possible metrological quality and deduces the pressure unit to the corresponding SI units. Primary standards for high and ultrahigh vacuum pressures are normally pressure generators, i.e., well-known pressures with a correlated uncertainty are generated in there. The methods of how the pressures can be generated have been reviewed in Ref. [44]. In the same book the procedures to calibrate ionization gauges have also been described. Primary standards for vacuum pressures are available in the major National Metrological Institutes of the world, among them the Physikalisch-Technische Bundesanstalt (PTB, Germany), the National Institute of Standards and Technology (NIST, USA), and the National Physical Laboratory (NPL, England).

## References

- [1] O. von Baeyer, *Phys. Z.* **10** (1909) 168.
- [2] O.E. Buckley, *Proc. Natl. Acad. Sci. USA* **2** (1916) 683.
- [3] R.T. Bayard and D. Alpert, *Rev. Sci. Instrum.* **21** (1950) 571.
- [4] F.M. Penning, *Physica* **4** (1937) 71, and *Philips Tech. Rev.* **2** (1937) 201.
- [5] P. A. Redhead, *Can. J. Phys.* **37** (1959) 1260.
- [6] J.P. Hobson and P.A. Redhead, *Can. J. Physics* **36** (1958) 271.
- [7] P.A. Redhead, J.P. Hobson and E.V. Kornelsen, *The Physical Basis of Ultrahigh Vacuum*, Chapman and Hall Ltd, London, 1968, p. 335.
- [8] B.R.F. Kendall and E. Drubetsky, *J. Vac. Sci. Technol. A* **18** (2000) 1724–1729.
- [9] R.N. Peacock and N.T. Peacock, *J. Vac. Sci. Technol. A* **8** (1990) 3341.
- [10] A. Van Oostrom, *Transactions of the Eighth Vacuum Symposium and Second International Congress* (Pergamon, Oxford, 1962), p. 443.
- [11] G. Comsa, *J. Appl. Phys.* **37** (1966) 554.
- [12] C. Benvenuti and M. Hauer, *Nucl. Instrum. Methods* **140** (1977) 453–460.
- [13] J. Groszkowski, *Bull. Acad. Polon. Sci. Ser. Sci. Technol.* **13** (1965) 2.
- [14] P.A. Redhead, *Rev. Sci. Instrum.* **31** (1960) 343.
- [15] P.A. Redhead, *Vacuum* **13** (1963) 253.
- [16] P.A. Redhead, *J. Vac. Sci. Technol. A* **12** (1994) 904–914.
- [17] J.P. Hobson, *J. Vac. Sci. Technol.* **1** (1964) 1.
- [18] [www.xtronic.ch](http://www.xtronic.ch) (Mai 2006).
- [19] J.C. Helmer and W.D. Hayward, *Rev. Sci. Instrum.* **37** (1966) 1652.
- [20] J. C. Helmer, *Vacuum* **51** (1998) 7–10.
- [21] C. Benvenuti and M. Hauer, *Proc. IVC-8, Cannes 1980, Suppl. à la Rev Le Vide, les Couches Minces* no. 201.
- [22] S.W. Han, W. Jitschin, P. Röhl and G. Grosse, *Vacuum* **38** (1988) 1079–1082.

- [23] B. Lagel, CERN Vacuum Technical Note 95-15, October 1995.
- [24] F. Watanabe, *J. Vac. Sci. Technol. A* **10** (1992) 3333.
- [25] J.M. Lafferty, *J. Appl. Phys.* **32** (1961) 424.
- [26] H. Akimichi *et al.*, *Vacuum* **46** (1995) 749–752.
- [27] J.H. Craig and J.H. Hock, *J. Vac. Sci. Technol.* **17** (1980) 1360–1363.
- [28] R. Baptist, *Vacuum* **48** (1997) 723–725, and R. Baptist and F. Bachelet, *Vacuum* **48** (1997) 947–951.
- [29] B. Bushan (ed.), *Springer Handbook of Nanotechnology* (Springer, Berlin, 2004), p. 74.
- [30] N.S. Xu and S. Ejaz Huq, *Mater. Sci. Eng. R* **48** (2005) 47–189.
- [31] W. Knapp and D. Schleufner, *Appl. Surf. Sci.* **251** (2005) 164–169.
- [32] P.G. Collins and A. Zettl, *Phys. Rev. B* **55** (1997) 9391–9399.
- [33] A.N. Obraztsov *et al.*, *J. Vac. Sci. Technol. B* **18** (2000) 1059–1063.
- [34] Detian Li and K. Jousten, *Vacuum* **70** (2003) 531–541.
- [35] Detian Li and K. Jousten, *J. Vac. Sci. Technol. A* **21** (2003) 937–946.
- [36] J. Miertusova, *Vacuum* **51** (1998) 61–68.
- [37] K. Jousten, *Vacuum* **49** (1998) 81.
- [38] D. Alpert, *Le Vide* **17** (1962) 19.
- [39] J.G. Werner and J.H. Leck, *J. Sci. Instrum. E* **2** (1969) 861–866.
- [40] J.H. Leck, *Total and Partial Pressure Measurement in Vacuum Systems* (Blackie, Glasgow and London, 1989), p.73.
- [41] R.L. Summers, *NASA Tech. Note NASA TN D-5285* (1969).
- [42] K. Jousten and P. Rohl, *Vacuum* **46** (1995) 9.
- [43] A. Berman, *Total Pressure Measurements in Vacuum Technology* (Academic Press, Orlando, FL, 1985), p. 45.
- [44] J.M. Lafferty, *Foundations of Vacuum Science and Technology* (John Wiley and Sons, New York, 1998), Chapter 12.

## Bibliography

- A. Berman, *Total Pressure Measurements in Vacuum Technology* (Academic Press, Orlando, FL, 1985).
- Saul Dushman, *Scientific Foundations of Vacuum Technique*, 2nd edition (John Wiley & Sons, New York, 1962).
- Karl Jousten, *Wutz Handbuch Vakuumtechnik*, 9<sup>th</sup> edition (Vieweg, Wiesbaden, 2006), ISBN 3-8348-0133-X.
- James M. Lafferty, *Foundations of Vacuum Science and Technology* (John Wiley & Sons, New York, 1998).
- J.H. Leck, *Total and Partial Pressure Measurement in Vacuum Systems* (Blackie, Glasgow, 1989).
- P.A. Redhead, J.P. Hobson and E.V. Kornelsen, *The Physical Basis of Ultrahigh Vacuum* (Chapman and Hall Ltd, London, 1968). This book has recently been re-edited by the American Vacuum Society.